

Molecular Physics

An International Journal at the Interface Between Chemistry and Physics

ISSN: 0026-8976 (Print) 1362-3028 (Online) Journal homepage: <https://www.tandfonline.com/loi/tmph20>

Quantum computing methods for electronic states of the water molecule

Teng Bian, Daniel Murphy, Rongxin Xia, Ammar Daskin & Sabre Kais

To cite this article: Teng Bian, Daniel Murphy, Rongxin Xia, Ammar Daskin & Sabre Kais (2019): Quantum computing methods for electronic states of the water molecule, Molecular Physics, DOI: [10.1080/00268976.2019.1580392](https://doi.org/10.1080/00268976.2019.1580392)

To link to this article: <https://doi.org/10.1080/00268976.2019.1580392>



Published online: 20 Feb 2019.



Submit your article to this journal [↗](#)



Article views: 46



View Crossmark data [↗](#)

Quantum computing methods for electronic states of the water molecule

Teng Bian^a, Daniel Murphy^b, Rongxin Xia^a, Ammar Daskin^c and Sabre Kais^{a,d}

^aDepartment of Physics and Astronomy, Purdue University, West Lafayette, IN, USA; ^bSchool of Physics, Georgia Institute of Technology, Atlanta, GA, USA; ^cDepartment of Computer Engineering, Istanbul Medeniyet University, Istanbul, Turkey; ^dDepartment of Chemistry, Purdue University, West Lafayette, IN, USA

ABSTRACT

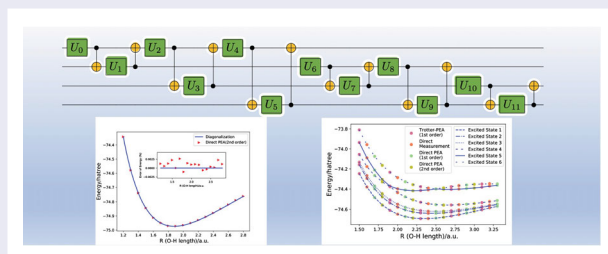
We compare recently proposed methods to compute the electronic state energies of the water molecule on a quantum computer. The methods include the phase estimation algorithm based on Trotter decomposition, the phase estimation algorithm based on the direct implementation of the Hamiltonian, direct measurement based on the implementation of the Hamiltonian and a specific variational quantum eigensolver, Pairwise VQE. After deriving the Hamiltonian using STO-3G basis, we first explain how each method works and then compare the simulation results in terms of gate complexity and the number of measurements for the ground state of the water molecule with different O–H bond lengths. Moreover, we present the analytical analyses of the error and the gate-complexity for each method. While the required number of qubits for each method is almost the same, the number of gates and the error vary a lot. In conclusion, among methods based on the phase estimation algorithm, the second-order direct method provides the most efficient circuit implementations in terms of the gate complexity. Moreover, Pairwise VQE serves the most practical method for near-term applications on the current available quantum computers. Finally the possibility of extending the calculation to excited states and resonances is discussed.

ARTICLE HISTORY

Received 14 September 2018
Accepted 22 January 2019

KEYWORDS

Water molecule; quantum computing methods; electronic states; resonances



1. Introduction

The problem at the heart of computational chemistry is electronic structure calculation. This problem concerns calculating the properties of the stationary state describing many electrons interacting with some external potential and between each other via Coulomb repulsion. The ability to efficiently solve these problems for the cases of many body systems can have huge effects in pharmaceutical development, materials engineering, and all areas of chemistry. Quantum computing proposes the possibility to efficiently solve this problem for molecules with many more electrons than what can currently be simulated by classical computers [1].

The ability to calculate properties of large quantum systems using precise control of some other quantum system was first proposed by Feynman [2]. He pointed out that if you have enough control over the states of some quantum system, you can create an analogy to some other quantum system. Using the example of spin in a lattice imitating many properties of bosons in quantum field theory, he conjectured that if you have enough individual quantum systems you could simulate any arbitrary quantum mechanical system. Simulation of the electronic structure Hamiltonian works very similar to this. Using the Jordan-Wigner or Bravyi-Kitaev transformation [3–5] you can map an electronic structure

Hamiltonian to a spin-type Hamiltonian which preserves energy eigenvalues [6]. Evolution under this spin-type Hamiltonian, e^{-iHt} , can then be approximately simulated on quantum computers.

Quantum simulation provides a new and efficient way to calculate eigenenergies of a given molecule. Classically the problem would have a computational cost which grows exponentially with the system size, n , the number of orbital basis functions [7]. However, based on the phase estimation algorithm [8,9], the molecular ground state energies can be calculated with gate depth $O(\text{poly}(n))$ [10–12]. The quantum circuit for the Hamiltonian is generally approximated through a Trotter–Suzuki decomposition. It is shown that the Hamiltonian dynamics can also be simulated through a truncated Taylor series [13]. This method is generalised as quantum signal processing [14]. Babbush *et al.* [15] further shows that it is possible to reduce the gate depth of the circuit to $O(n)$ by using plane wave orbitals. Recently, a direct circuit implementation of the Hamiltonian within the phase estimation (Direct-PEA) is presented by authors of paper [16–18]: the circuit designs are provided to the time evolution operator by using the truncated series such as $U = I - iH/\kappa$ and $U = tH + i(I - t^2H^2/2)$, in which κ and t are parameters to restrict truncation error. These unitary operators are much simpler to implement than those of a Trotter decomposition, and can be also used to calculate ground state energies of molecular Hamiltonians. Another approach called variational quantum eigensolver (VQE) has been introduced by Aspuru-Guzik and coworkers [19,20]: This method combines classical and quantum algorithms together and significantly reduces the gate complexity at the cost of a large amount of measurements. It has also been applied on real-world quantum computers to solve ground state energies of molecules such as: H_2 , LiH and BeH_2 [21,22].

This paper explores all these above mentioned methods for calculating the ground state energies of the water molecule and presents a comparison study, in terms of both the accuracy and the gate complexity dependent on error. The next section explains the method by which the electronic Hamiltonian for water is calculated and the method by which to reduce the number of qubits required to simulate the transformed spin-type Hamiltonian. Then, Section 3 discusses five methods of electronic structure simulation on quantum computers: the phase estimation using first-order Trotter–Suzuki decomposed propagator (Trotter PEA), two direct implementations of the spin-type Hamiltonian (Direct PEA), a direct measurement and a specific variational quantum eigensolver method (Pairwise VQE). Section 4 shows results for these methods with comparison to the exact energy from direct diagonalisation of the spin-type Hamiltonian. It also

gives qubit requirement and gate complexity for different methods asymptotically. Spin-type Hamiltonian for H_2O at equilibrium bond length is derived in Appendix 1. Details of both error and complexity analyses are given in Appendices 2 and 3.

2. Hamiltonian derivation

In this section we provide details for calculating the spin-type Hamiltonian describing electronic structures of the water molecule using STO-3G basis set that will be used in later methods. This derivation can be generalised to an arbitrary molecular Hamiltonian.

To obtain the Hamiltonian of the water molecule, we start by considering the 1s orbital of each hydrogen atom along with the 1s, 2s, 2p_x, 2p_y, 2p_z orbitals for the oxygen atom. This leads to a total of 14 molecular orbitals considering spin. To make our simulations more efficient, the number of qubits is reduced by considering orbital energies and exploiting the symmetry of the system [22].

It can be initially assumed that the two molecular orbitals of largest energies are unoccupied. Consequently, the calculation of the Hamiltonian of the water molecule then only requires the consideration of 12 spin-orbitals. After second quantisation, the Hamiltonian can be expressed as [23]:

$$H = \sum_{i,j=1}^{12} h_{ij} a_i^\dagger a_j + \frac{1}{2} \sum_{i,j,k,l=1}^{12} h_{ijkl} a_i^\dagger a_j^\dagger a_k a_l. \quad (1)$$

Here a_i^\dagger and a_i are fermionic creation and annihilation operators, and $h_{i,j}$ and $h_{i,j,k,l}$ are one-body and two-body interaction coefficients. In this work the molecular orbitals are calculated from the Hartree-Fock method and represented by the STO-3G basis functions. The numerical integration obtaining the one and two electron integrals for molecular water is performed by the PyQuante package [24]. The expressions for these integrations are:

$$h_{ij} = \int d\vec{r}_1 \chi_i^*(\vec{r}_1) \left(-\frac{1}{2} \nabla_1^2 - \sum_{\sigma} \frac{Z_{\sigma}}{|\vec{r}_1 - \vec{R}_{\sigma}|} \right) \chi_j(\vec{r}_1), \quad (2)$$

$$h_{ijkl} = \int d\vec{r}_1 d\vec{r}_2 \chi_i^*(\vec{r}_1) \chi_j^*(\vec{r}_2) \frac{1}{r_{12}} \chi_k(\vec{r}_2) \chi_l(\vec{r}_1). \quad (3)$$

Here we have defined $\chi_i(\vec{r})$ as the i th spin-orbital, which is calculated from a spatial orbital obtained by the Hartree-Fock method and the electron spin states. Z_{σ} is the σ th nuclear charge, \vec{r}_i is the position of electron i , r_{12} is the distance between the two points r_1 and r_2 , and \vec{R}_{σ} is the position of σ th nucleus.

We have ordered our spin-orbitals from 1 to 12 as follows: $\{1 \uparrow, 2 \uparrow, \dots, 6 \uparrow, 1 \downarrow, 2 \downarrow, \dots, 6 \downarrow\}$, with first spin-up orbitals ordered from lowest to highest energy and continuing into spin-down orbitals ordered from lowest to highest energy. Now introduce an ad hoc set $F = \{1, 2, 7, 8\}$ corresponding to the 4 lowest energy spin orbitals $\{1 \uparrow, 2 \uparrow, 1 \downarrow, 2 \downarrow\}$. For the H_2O ground state, it can be assumed the spin orbitals in the set F will be filled with electrons. The following one-body single electron interaction operators then become:

$$\begin{aligned} a_1^\dagger a_1 &= 1, & a_2^\dagger a_2 &= 1, & a_7^\dagger a_7 &= 1, & a_8^\dagger a_8 &= 1, \\ a_i^\dagger a_j &= 0, & \text{if } i \neq j & \text{ and } & i \in F \text{ or } j \in F. \end{aligned} \quad (4)$$

This assumption also allows us to simplify the two-electron interaction terms under certain conditions:

$$a_i^\dagger a_j^\dagger a_k a_l = \begin{cases} a_j^\dagger a_k, & i = l, i \in F, \{j, k\} \notin F, \\ a_i^\dagger a_l, & j = k, j \in F, \{i, l\} \notin F, \\ -a_j^\dagger a_l, & i = k, i \in F, \{j, l\} \notin F, \\ -a_i^\dagger a_k, & j = l, j \in F, \{i, k\} \notin F. \end{cases} \quad (5)$$

Moreover, this ability to neglect creation or annihilation operator with subscript from $\{1, 2, 7, 8\}$, along with the ability to neglect two-body operators containing an odd number of modes in F , allows us to relabel our orbital set 1 to 8, corresponding to spin-orbitals: $\{3 \uparrow, 4 \uparrow, 5 \uparrow, 6 \uparrow, 3 \downarrow, 4 \downarrow, 5 \downarrow, 6 \downarrow\}$

Using the parity basis and taking advantage of particle and spin conversation, the required qubit number can be further reduced [25]. In the parity basis:

$$a_j^\dagger = X_{j+1}^{\leftarrow} \otimes \frac{1}{2}(X_j \otimes Z_{j-1} - iY_j), \quad (6)$$

$$a_j = X_{j+1}^{\leftarrow} \otimes \frac{1}{2}(X_j \otimes Z_{j-1} + iY_j), \quad (7)$$

where

$$X_i^{\leftarrow} \equiv X_{n-1} \otimes X_{n-1} \otimes \dots \otimes X_{i+1} \otimes X_i, \quad n = 8. \quad (8)$$

This fermionic Hamiltonian can now be mapped to an 8-local Hamiltonian represented as a weighted sum of tensor products of Pauli matrix $\{I_i, X_i, Y_i, Z_i\}$, which almost preserves the ground state energy value. The new Hamiltonian in the electronic occupation number basis set can be mapped to the parity basis set as:

$$|f_1 f_2 \dots f_8\rangle \rightarrow |q_1\rangle \otimes |q_2\rangle \otimes \dots \otimes |q_8\rangle, \quad (9)$$

where

$$q_i = \sum_{k=1}^i f_k \bmod 2 \in \{0, 1\}. \quad (10)$$

Here f_k represents the number of electrons occupying the k th spin-orbital, and q_k represents the sum of electron numbers from 1st to k th spin-orbital.

We can now assume that half of the left 6 electrons are spin-up and the other half are spin-down. If this is the case, $|q_4\rangle = |1\rangle$, and $|q_8\rangle = |0\rangle$, which means only Z_4, I_4, Z_8, I_8 will apply on these states [26]. Since $Z_4 |q_4\rangle = -|q_4\rangle, Z_8 |q_8\rangle = |q_8\rangle$, all Z_4, Z_8 can be substituted by $-I_4$ and I_8 , with this assumption we can now reduce this problem to a 6-local Hamiltonian.

3. Methods of simulation

After the parity transformation and simplifications made above we now have a reduced 6-local Hamiltonian describing H_2O in the form: $H = \sum_{i=1}^L \alpha_i h_i$, where $\{\alpha_i\}$ is a set of coefficients, and $\{h_i\}$ is a set of tensor products of the Pauli matrices $\{I_i, X_i, Y_i, Z_i\}$. Method A,B,C tries to evolve quantum system state by approximating the propagator e^{-iHt} , and then extract the ground state energy from the phase. Method D implements the Hamiltonian, H , directly into quantum circuit, and evaluate ground state energy by multiple measurements. Method E produces the ground state energies by iterations.

3.1. Trotter phase estimate algorithm (Trotter-PEA)

For each term in a Hamiltonian, H , the propagator, $e^{-i\alpha_i h_i t}$, can be easily constructed in a circuit. However, since most of the time the set of h_i do not commute, the propagator cannot be implemented term by term: i.e. $e^{-iHt} \neq \prod_{i=1}^L e^{-i\alpha_i h_i t}$. The first-order Trotter-Suzuki decomposition [27–29] provides an easy way to decompose a propagator for the spin-type Hamiltonian given as a sum of non-commuting terms into a product of each non-commuting term exponentiated for a small time t :

$$U = \prod_{i=1}^L e^{-i\alpha_i h_i t} = e^{-iHt} + O(A^2 t^2). \quad (11)$$

Here $A = \sum_{i=1}^L |\alpha_i|$, and we have an error of order $O(A^2 t^2)$. Here we don't consider time slicing as the original Trotter-Suzuki decomposition does, as t can be adjusted to be as small as necessary for error control. This method requires only multi-qubit rotations, and therefore U can be implemented easily on a state register.

After U is obtained PEA can be applied to extract the phase. We can use extra ancilla qubits to achieve wanted accuracy by iterative measurements [10,30,31]. We call this PEA based on first-order Trotter-Suzuki decomposition Trotter-PEA.

Higher order Trotter-Suzuki decompositions are also available, however they have more complicated formulations, especially for order higher than 2. Here we only discuss first-order case for simplicity. For simulation, a forward iterative PEA [18] – which estimates the phase

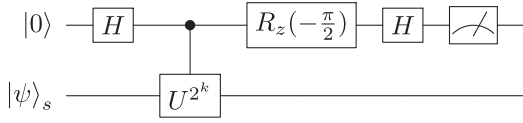


Figure 1. Forward iterative PEA circuit with initial state $|0\rangle | \psi \rangle_s$. Here $| \psi \rangle_s$ is the ground state of the Hamiltonian, H is the Hadamard gate, U is the approximate propagator and $R_z(-\pi/2)$ is a Z rotation gate.

starting from the most significant bit-can be used to save more time. The circuit for the forward iterative PEA is shown in Figure 1 which needs only 1 qubit for measurement. Then the generated state before the measurement is:

$$\frac{1 + e^{i2\pi(0.\phi_{k+1}\phi_{k+2}\dots-0.01)}}{2} e^{i(\pi/4)} |0\rangle | \psi \rangle_s + \frac{1 - e^{i2\pi(0.\phi_{k+1}\phi_{k+2}\dots-0.01)}}{2} e^{i(\pi/4)} |1\rangle | \psi \rangle_s. \quad (12)$$

Note decimals above are in binary. It can be checked if the measurement qubit has a greater probability of output 1, $\phi_{k+1} = 1$, otherwise $\phi_{k+1} = 0$. Then the ground state energy can be calculated as $E = -2\pi \times 0.\phi_1\phi_2\phi_3\dots$

3.2. Direct implementation of hamiltonian in first-order (Direct-PEA (1st order))

It was proposed [17] that given a Hamiltonian H and large κ we can construct an approximated unitary operator U such that:

$$U = I - i\frac{H}{\kappa}, \quad \kappa \gg \sum_{i=1}^L |\alpha_i| \geq \|H\|. \quad (13)$$

If $| \psi \rangle_s$ is an eigenvector of H and E is the corresponding eigenvalue, then:

$$U | \psi \rangle_s = \left(I - i\frac{H}{\kappa} \right) | \psi \rangle_s \approx e^{-i(H/\kappa)} | \psi \rangle_s = e^{-i(E/\kappa)} | \psi \rangle_s. \quad (14)$$

The eigenvalue of $| \psi \rangle_s$ would be encoded directly in the approximate phase. This is the motivation behind directly implementing the Hamiltonian in quantum simulation.

To implement this non-unitary matrix U , we can enlarge the state space and construct a unitary operator U_r [13]. Rewrite U as:

$$U = I - \frac{i}{\kappa} \sum_{j=1}^L \alpha_j h_j = \sum_{j=0}^L \beta_j V_j, \quad (15)$$

in which $\beta_j \geq 0$ and V_j is unitary. By introducing a m -qubit ancilla register, where $m = \lceil \log_2 L \rceil$, we can construct a multi-control gate, V , such that:

$$V | j \rangle_a | \psi \rangle_s = | j \rangle_a V_j | \psi \rangle_s. \quad (16)$$

Define $\beta_j = 0$ when $L < j \leq 2^m$ and B as a unitary operator that acts on ancilla qubits as:

$$B | 0 \rangle_a = \frac{1}{\sqrt{s}} \sum_{j=0}^{2^m} \sqrt{\beta_j} | j \rangle_a, \quad s = \sum_{j=0}^{2^m} \beta_j. \quad (17)$$

Define U_r and Π such that:

$$U_r = (B^\dagger \otimes I^{\otimes n}) V (B \otimes I^{\otimes n}), \quad (18)$$

$$\Pi = | 0 \rangle_a \langle 0 |_a \otimes I^{\otimes n}. \quad (19)$$

Apply U_r on input state $| 0 \rangle_a | \psi \rangle_s$:

$$\begin{aligned} U_r | 0 \rangle_a | \psi \rangle_s &= (B^\dagger \otimes I^{\otimes n}) V (B \otimes I^{\otimes n}) | 0 \rangle_a | \psi \rangle_s \\ &= (B^\dagger \otimes I^{\otimes n}) V \frac{1}{\sqrt{s}} \sum_{j=0}^{2^m} \sqrt{\beta_j} | j \rangle_a | \psi \rangle_s \\ &= (B^\dagger \otimes I^{\otimes n}) \frac{1}{\sqrt{s}} \sum_{j=0}^{2^m} \sqrt{\beta_j} | j \rangle_a V_j | \psi \rangle_s \\ &= \Pi (B^\dagger \otimes I^{\otimes n}) \frac{1}{\sqrt{s}} \sum_{j=0}^{2^m} \sqrt{\beta_j} | j \rangle_a V_j | \psi \rangle_s \\ &\quad + (I^{\otimes m+n} - \Pi) (B^\dagger \otimes I^{\otimes n}) \frac{1}{\sqrt{s}} \\ &\quad \times \sum_{j=0}^{2^m} \sqrt{\beta_j} | j \rangle_a V_j | \psi \rangle_s \\ &= (B | 0 \rangle_a \langle 0 |_a)^\dagger \frac{1}{\sqrt{s}} \sum_{j=0}^{2^m} \sqrt{\beta_j} | j \rangle_a V_j | \psi \rangle_s \\ &\quad + \sum_{j=1}^{j=2^m} | j \rangle_a | u_j \rangle_s \\ &= \frac{1}{s} | 0 \rangle_a U | \psi \rangle_s + | \Phi_1^\perp \rangle, \quad (20) \end{aligned}$$

where $| \Phi_1^\perp \rangle$ is orthogonal to $| 0 \rangle_a | \psi \rangle_s$. Then the approximated unitary operator U is implemented by unitary operator U_r , which can be seen in Figure 2. Since $\kappa \gg \|H\| \geq E$, energy of eigenstate $| \psi \rangle_s$ is successfully

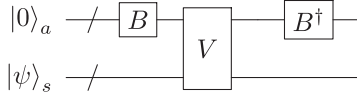


Figure 2. Gate U_r indirect PEA circuit, gates V and B are shown in Equations (16) and (17).

implemented in phase:

$$\begin{aligned} U_r |0\rangle_a |\psi\rangle_s &= \frac{1 - i\frac{E}{\kappa}}{s} |0\rangle_a |\psi\rangle_s + |\Phi_1^\perp\rangle \\ &= \frac{\sqrt{1 + \frac{E^2}{\kappa^2}}}{s} e^{-i \tan^{-1}(E/\kappa)} |0\rangle_a |\psi\rangle_s + |\Phi_1^\perp\rangle \\ &= p e^{-i \tan^{-1}(E/\kappa)} |0\rangle_a |\psi\rangle_s + \sqrt{1 - p^2} |\Phi_1^\perp\rangle. \end{aligned} \quad (21)$$

Here p is defined by $\sqrt{1 + E^2/\kappa^2}/s$, and $|\Phi_1^\perp\rangle$ is normalised.

This U_r gate would then be used for PEA or iterative PEA process. For an accurate output, p is required to be as close to 1 as possible. Using oblivious amplitude amplification [32], we can amplify that probability without affecting phase. Define the operator $U_0 = 2 |0\rangle_a \langle 0_a - I^{\otimes m}$ and rotational operator:

$$Q = U_r (U_0 \otimes I^{\otimes n}) U_r^\dagger (U_0 \otimes I^{\otimes n}). \quad (22)$$

Iterating this operator N times, we can achieve $U_q = Q^N U_r$ which brings p close to 1 by performing rotations within the space $\text{span}\{|0\rangle_a |\psi\rangle_s, |\Phi_1^\perp\rangle\}$. The details are in Supplementary Materials. Take the same circuit and the same procedure in Trotter-PEA, except replacing U by U_q , we are able to get ground state energy of water molecule.

3.3. Direct implementation of hamiltonian in second-order (Direct-PEA (2nd order))

Propagator e^{-iHt} can also be approximated up to second order [18]:

$$U = I - iHt - \frac{H^2 t^2}{2} = e^{-iHt} + O((At)^3). \quad (23)$$

When At is very small, U would be a good approximation. Since U is non-unitary, we have to construct a unitary operator U_{r2} to implement it into a quantum circuit. With U_r in method B, B_2 defined with the property:

$$B_2 |00\rangle = \frac{\sqrt{t} |00\rangle + |01\rangle + \frac{t}{\sqrt{2}} |10\rangle}{\sqrt{1 + t + \frac{t^2}{2}}}, \quad (24)$$

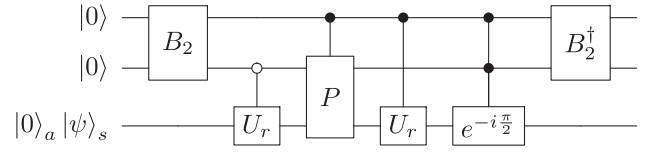


Figure 3. Gate U_{r2} in second-order direct PEA circuit, with B_2 and P defined in Equations (24) and (25).

and gate P constructed as:

$$P = \begin{bmatrix} I^{\otimes n} & 0 & 0 & 0 \\ 0 & 0 & I^{\otimes m} & 0 \\ 0 & I^{\otimes m} & 0 & 0 \\ 0 & 0 & 0 & I^{\otimes n} \end{bmatrix}. \quad (25)$$

We can construct U_{r2} as in Figure 3: which satisfies:

$$\begin{aligned} U_{r2} |00\rangle |0\rangle_a |\psi\rangle_s &= \frac{1 - i\frac{Et}{A} + \frac{E^2 t^2}{2A^2}}{1 + t + \frac{t^2}{2}} |00\rangle |0\rangle_a |\psi\rangle_s + \sum_{j=1}^{2^{m+2}} |j\rangle |v_j\rangle_s \\ &= \frac{\sqrt{1 + \frac{E^4 t^4}{4A^2}}}{1 + t + \frac{t^2}{2}} e^{-i \tan^{-1}((Et/A)/(1 + E^2 t^2/2A))} |00\rangle |0\rangle_a |\psi\rangle_s + |\Psi_1^\perp\rangle. \end{aligned} \quad (26)$$

In the formula, $A = \sum_{i=1}^{2^m-1} \beta_i = \sum_{i=1}^L |\alpha_i| \geq |E|$, and $|\Psi_1^\perp\rangle$ is perpendicular to $|00\rangle |0\rangle_a |\psi\rangle_s$. Just as in last section, we can rotate the final state to make the proportion of $|00\rangle |0\rangle_a |\psi\rangle_s$ as close to 1 as possible. Then we can apply PEA or iterative PEA to get the phase, $-\tan^{-1}((Et/A)/(1 + E^2 t^2/2A))$, which leads to ground state energy corresponding to ground state $|\psi\rangle_s$.

3.4. Direct measurement of Hamiltonian

Another way to calculate the ground state energy is by direct measurement after implementing a given Hamiltonian as a circuit. Since Direct-PEA (1st order) method has already introduced a way to implement non-unitary matrix U into circuit, Hamiltonian implementation is straightforward. We can just replace U in method B by $U' = H = \sum_{j=1}^L \alpha_j h_j$, and obtain U'_r such that:

$$\begin{aligned} U'_r |0\rangle_a |\psi\rangle_s &= \frac{1}{s'} |0\rangle_a U'_r |\psi\rangle_s + |\Phi_1'^\perp\rangle \\ &= \frac{E}{A} |0\rangle_a |\psi\rangle_s + |\Phi_1'^\perp\rangle. \end{aligned} \quad (27)$$

By measuring ancilla qubits multiple times, we can get the energy of the ground state $|\psi\rangle_s$ by multiplying A by the square root of probability of getting all 0s.

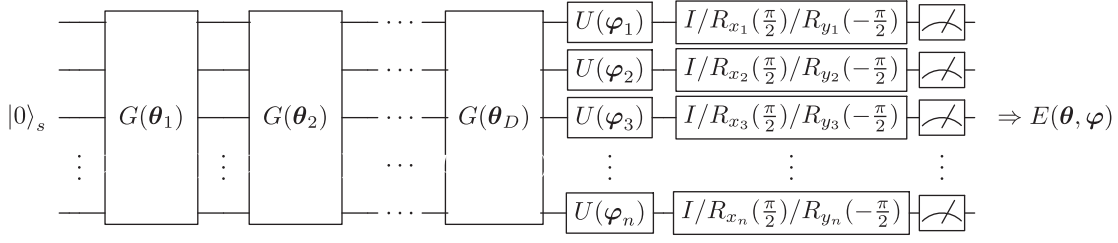


Figure 4. Circuit for state preparation and corresponding energy evaluation. $G(\theta_i)$ is entangling gate, in this paper we are taking the gate like Figure 5. $U(\varphi_k)$ is an arbitrary single-qubit rotation and is equal to $R_z(\varphi_{k,1})R_x(\varphi_{k,2})R_z(\varphi_{k,3})$ with parameters $\varphi_{k,1}, \varphi_{k,2}$ and $\varphi_{k,3}$ that can be manipulated. By increasing the number of layers, d , of our circuit, we are able to produce more complex states.

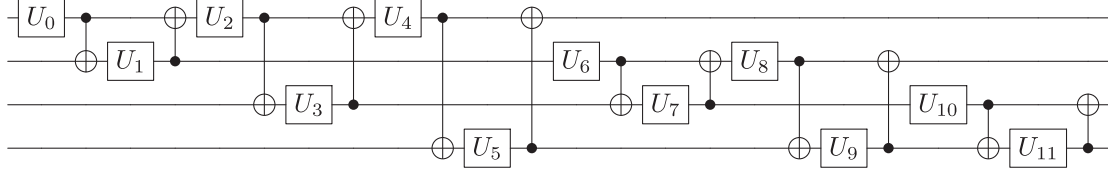


Figure 5. Example entangling circuit $G(\theta_i)$ for 4-qubit system. There are 12 arbitrary single-qubit gates U_j , a simplified written way for $U(\theta_{ij})$, which is $R_z(\theta_{ij,1})R_x(\theta_{ij,2})R_z(\theta_{ij,3})$ with parameters $\theta_{ij,1}, \theta_{ij,2}$ and $\theta_{ij,3}$ that can be manipulated. Each 2 qubits are entangled sequentially. Entangling gate $G(\theta_i)$ for n -qubit system is similar to this gate, but then it has $n(n-1)$ arbitrary single-qubit gates and θ_i has $3n(n-1)$ parameters.

This method can also be used for non-hermitian Hamiltonians. If now the eigenvalue for $|\psi\rangle_s$ is a complex number $E = |E|e^{i\theta}$, by replacing U by $U' = H$ in method B, we would have:

$$U'_r |0\rangle_a |\psi\rangle_s = \frac{|E|e^{i\theta}}{A} |0\rangle_a |\psi\rangle_s + |\Phi_1^\perp\rangle, \quad (28)$$

and can obtain $|E|$ through measurements. Then by replacing U by $U'' = (|E|/A)I + H$ in method B, we would have:

$$U''_r |0\rangle_a |\psi\rangle_s = \frac{|E|}{A} (1 + e^{i\theta}) |0\rangle_a |\psi\rangle_s + |\Phi_1^\perp\rangle, \quad (29)$$

and can measure the absolute value of $(|E|/A)(1 + e^{i\theta})$, which is $2(|E|/A) \cos \theta$. This helps determine the phase of a complex eigenenergy.

3.5. Variational quantum eigensolver

Recently the variational quantum eigensolver method has been put forward by Aspuru-guzik and coworkers to calculate the ground state energies [19–22,33], which is a hybrid method of classical and quantum computation. According to this method, an adjustable quantum circuit is constructed at first to generate a state of the system. This state is then used to calculate the corresponding energy under the system's Hamiltonian. Then by a classical optimisation algorithm, like Nelder–Mead method, parameters in circuit can be adjusted and the generated state will be updated. Finally, the minimal energy will be obtained. The detailed circuit for the quantum part of our algorithm

is shown in Figure 4. To make the expression more clear, we represent parameters in vector form, as follows: $\theta = (\theta_1, \theta_2, \dots, \theta_D)$, $\theta_i = (\theta_{i,0}, \theta_{i,1}, \dots, \theta_{i,11})$, $\theta_{ij} = (\theta_{ij,1}, \theta_{ij,2}, \theta_{ij,3}, \dots)$, $\varphi = (\varphi_1, \varphi_2, \dots, \varphi_n)$, $\varphi_k = (\varphi_{k,1}, \varphi_{k,2}, \varphi_{k,3}, \dots)$. We are using d layers of gate $G(\theta_i)$ in Figure 4 to entangle all qubits together. Here we introduce a hardware-efficient $G(\theta_i)$, and we call this method Pair-wise VQE. The example gate of $G(\theta_i)$ for 4 qubits is shown in Figure 5. The entangling gate for 6-qubit system H_2O is similar: every 2 qubits are modified by single-qubit gates and entangled by CNOT gate. By selecting initial value of all θ_i and φ_k , system state can be prepared by d layers $G(\theta_i)$ gates and arbitrary single gates $U(\varphi_j)$. Then average value of each term in Hamiltonian H , $\langle h_j \rangle$, can be evaluated by measuring qubits many times after going through gates like I or $R_{x_j}(\pi/2)$ or $R_{y_j}(-\pi/2)$. For example, if $h_j = I_0 X_1 Y_2 Z_3$, then

$$\begin{aligned} \langle h_j \rangle &= \langle I_0 X_1 Y_2 Z_3 \rangle_\psi = \langle \psi | I_0 X_1 Y_2 Z_3 | \psi \rangle \\ &= \left(\langle \psi | R_{y_1} \left(\frac{\pi}{2} \right) R_{x_2} \left(-\frac{\pi}{2} \right) \right) I_0 \left(R_{y_1} \left(-\frac{\pi}{2} \right) X_1 \right. \\ &\quad \left. R_{y_1} \left(\frac{\pi}{2} \right) \right) \left(R_{x_2} \left(\frac{\pi}{2} \right) Y_2 R_{x_2} \left(-\frac{\pi}{2} \right) \right) \\ &\quad \left. Z_3 \left(R_{y_1} \left(-\frac{\pi}{2} \right) R_{x_2} \left(\frac{\pi}{2} \right) | \psi \rangle \right) \right) \\ &= \langle I_0 Z_1 Z_2 Z_3 \rangle_{\psi'}, \quad \text{where } | \psi' \rangle \\ &= R_{y_1} \left(-\frac{\pi}{2} \right) R_{x_2} \left(\frac{\pi}{2} \right) | \psi \rangle, \end{aligned}$$

So we can let the quantum state after $U(\varphi_j)$ go through gates $R_{y_1}(-\pi/2)$ and $R_{x_2}(\pi/2)$ and then measure the

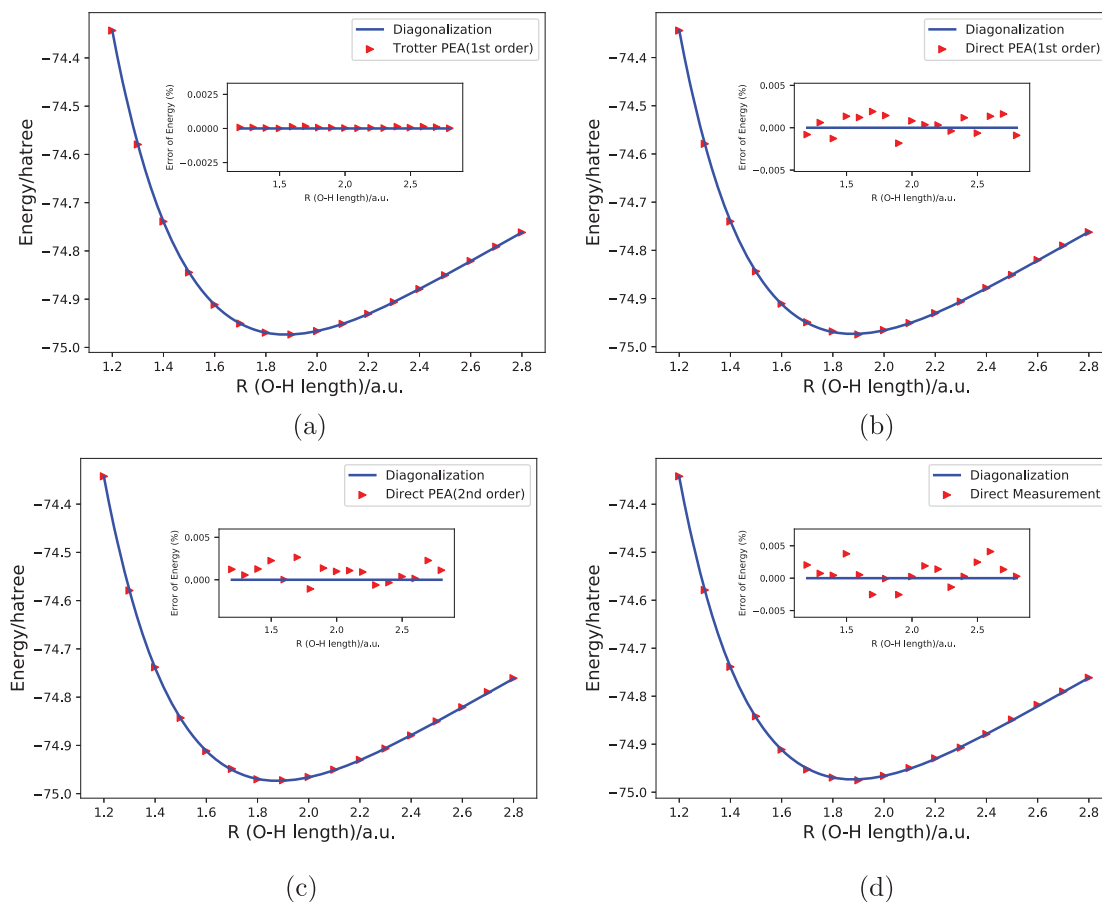


Figure 6. Ground State Energy Curve for H₂O, as a function of the bond length O–H in a.u. for (a) the Trotter-PEA, (b) the Direct-PEA (1st order), (c) the Direct-PEA (2nd order) and (d) Direct Measurement method (1.6×10^8 measurements), compared with the exact diagonalisation. Errors are shown in the window of each figure. One thing to mention is that we can not tell whether one method have better property over another directly from these figures, because they have different parameters, gates etc. For comparison, we have to turn to gate complexity analysis in Table 1.

result state multiple times to get $\langle h_j \rangle$. The energy corresponding to the state can be obtained by $\langle H \rangle(\theta, \varphi) = \sum_{j=1}^L \alpha_j \langle h_j \rangle(\theta, \varphi)$. Then θ and φ can be updated by classical optimisation method and $\langle H \rangle(\theta, \varphi)$ can reach the minimal step by step.

4. Results and method comparison

The Hamiltonian of the water molecule is calculated for O–H bond lengths ranging from 0.5 a.u. to 2.9 a.u., using the methods introduced in Section 2. This Hamiltonian is used in all five of the methods discussed within this paper. For the methods A–D, the input state of system is the ground state of the H₂O molecule. For each of these methods, the resulting ground state energy curve can be calculated to arbitrary accuracy (for details of error analysis see Appendix 2). The results from each method is compared with result from a direct diagonalisation of the Hamiltonian, as shown below. From Figure 6 it can be seen that all of these methods are effective in obtaining the ground state energy problem of the water molecule.

We also use method E (Pairwise VQE) to obtain the ground state energy. These results can be seen in Figure 7. Energy convergence at 1.9 a.u. can be seen in Figure 7(a) and the ground state energy curve calculated by this method is in Figure 7(b). In this simulation, d is selected to be 1, and $G(\theta_i)$ is constructed as described above, and it can already give a very accurate result. This shows Pairwise VQE a very promising method for solving electronic structure problems. Furthermore, Pairwise VQE has only $O(n^2d)$ gate complexity and doesn't require initial input of the ground state, which makes it more practical for near-term applications on a quantum computer.

Qubit requirement, gate complexity and number of measurements of different methods are analysed in Appendix 3 and shown in Table 1. When counting gate complexities, we decompose all gates into single qubit gates and CNOT gates. While Pairwise VQE needs only n qubits, the other methods require extra number of qubits. In terms of gate scaling, Pairwise VQE also needs the least gates, which enables it to better suit the applications on near and intermediate term quantum computers.

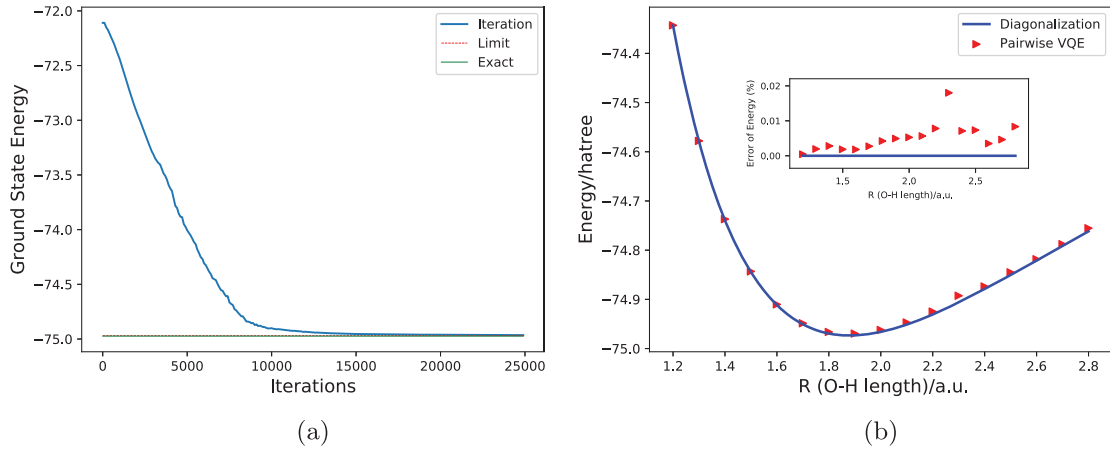


Figure 7. Result from Pairwise VQE using the entangling gates in Figure 5. We take $|0\rangle_s$ as initial input, $d = 1$ layer and use Nelder–Mead algorithm for optimisation. (a) Convergence of ground state energy of H_2O for fixed O–H bond length = 1.9 a.u., as number of iterations increases. The lines for exact ground state energy and for the limit almost overlap and (b) Ground state energy curve for H_2O , as a function of O–H bond length in a.u. for variational quantum eigensolver. Errors are shown in the window of the figure.

Table 1. Complexity of different methods.

Method	Qubits requirement	Gate complexity	Number of measurements
Trotter-PEA	$O(n)$	$O(\frac{n^5}{(\epsilon/A)^2})$	$O(1)$
Direct-PEA(1st order)	$O(n)$	$O(\frac{n^5}{(\epsilon/A)^{2.5}})$	$O(1)$
Direct-PEA(2nd order)	$O(n)$	$O(\frac{n^5}{(\epsilon/A)^{3.3}})$	$O(1)$
Direct measurement	$O(n)$	$O(n^5)$	$O(\frac{E^2}{\epsilon^2})$
Pairwise VQE	n	$O(n^2d)$	$O(\frac{A^2n^8}{\epsilon^2}N_{\text{iter}})$

Notes: n is the number of qubits for molecular system, 6 for water in this paper. $A = \sum_{i=1}^L |\alpha_i|$ can serve as the scale of energy. E is the exact value of ground energy. ϵ is the accuracy of energy we want to reach. d is the number of layers we used in Pairwise VQE. N_{iter} is the number of iterations for optimisation in Pairwise VQE. See Appendix 3 for details.

Among the remaining four methods, Direct Measurement requires less number of gates than the others. PEA-type methods have an advantage that they can give an accurate result under only $O(1)$ measurements. However, they need more qubits compared with the previous two methods and demands many more gates if smaller error is required. Due to huge gate complexity, these PEA-type algorithms would be put into practice only when the decoherence problem has been better solved. Among these three PEA-based methods, in terms of the gate complexity, Direct-PEA(2nd order) requires less number of gates than the traditional Trotter-PEA and Direct-PEA(1st order) which is proved in Appendix 3. One more thing to mention is that here the second quantisation form Hamiltonian is based on STO-3G, so there are $O(n^4)$ terms. If a more recent dual form of plane wave basis [15] is used, the number of terms can be reduced to $O(n^2)$, and the asymptotic scaling in Table 1 would also be reduced. To be specific, for PEA-type methods, upper bounds of gate complexities would be proportional to n^3

rather than n^5 , and Number of Measurements for Pairwise VQE would be proportional to n^4 rather than n^8 . As can be seen, these reductions wouldn't influence the comparison made above.

5. Excited states and resonances

All the aforementioned methods can also be applied for the excited state energy calculation. For PEA-type methods and Direct Measurement method, it can be simply done by replacing the input system state by an excited state. The complexity for the calculation is the same. The energy accuracies for excited states are also similar to that for the ground state. For VQE, a recent publication [34,35] presents a quantum subspace expansion algorithm (QSE) to calculate excited state energies. They approximate a 'subspace' of low-energy excited states from linear combinations of states of the form $O_i |\psi\rangle_s$, where $|\psi\rangle_s$ is the ground state determined by VQE and O_i are chosen physically motivated quantum operators. By diagonalising the matrix with elements $\langle \psi_s O_i^\dagger H O_j | \psi_s \rangle$ calculated by VQE, one is able to find the energies of excited states.

Figure 8 shows the simulation of the first six excited states' energy curves of the water molecule from our 6-qubit Hamiltonian, calculated by PEA-type methods and Direct Measurement method. It can be seen that the 5th excited energy curve indicates a shape resonance phenomenon, which can be described by a non-Hermitian Hamiltonian with complex eigenvalues. The life time of the resonance state is associated with the imaginary part of the eigenvalues. In this way, to solve the resonance problem, we can seek to solve the eigenvalues of non-Hermitian Hamiltonians.

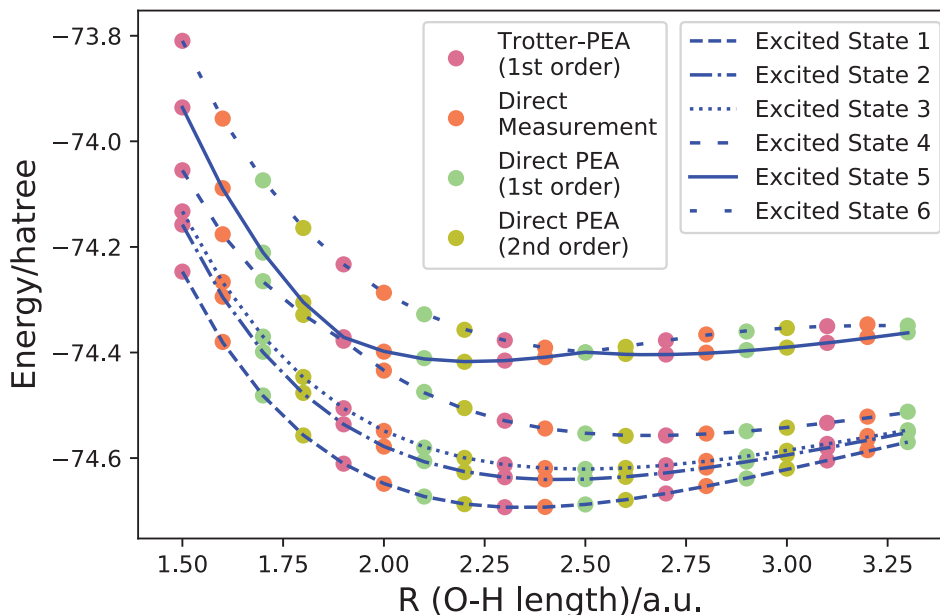


Figure 8. Excited states' energy curves for H_2O , as a function of the bond length O-H in a.u.. Markers with different colours represent data points calculated from different methods. Only a few points for each method are drawn for illustration. Energy curves in different line styles are calculated from exact diagonalisation of Hamiltonian matrix.

Some work has been done on this track to solve the resonance problem by quantum computers. By designing a general quantum circuit for non-unitary matrices, Daskin *et al.* [36] explored the resonance states of a model non-Hermitian Hamiltonian. To be specific, he introduced a systematic way to estimate the complex eigenvalues of a general matrix using the standard iterative phase estimation algorithm with a programmable circuit design. The bit values of the phase qubit determines the phase of eigenvalue, and the statistics of outcomes of the measurements on the phase qubit determines the absolute value of the eigenvalue. Other approaches for solving complex eigenvalues can also be applied for this resonance problem. For example, Wang *et al.* [37] proposed a measurement-based quantum algorithms for finding eigenvalues of non-unitary matrices. Terashima and Ueda [38] introduced a universal non-unitary quantum circuit by using a specific type of one-qubit non-unitary gates, the controlled-NOT gate, and all one-qubit unitary gates, which is also useful for finding the eigenvalues of a non-hermitian Hamiltonian matrix.

Method D in Section 3 can also be used for solving complex eigenvalues and the complexity is polynomial in system size. After applying complex-scaling method [39] to water molecule's Hamiltonian and obtaining a non-Hermitian Hamiltonian, we can make enough quantum measurements to get an accurate resonance width Γ , which is actually the imaginary part of Hamiltonian's eigenvalue [40]. Another easier way to solve this resonance problem is, we can first choose proper a and J to

fit the potential energy in a widely studied Hamiltonian [41–43]:

$$H(x) = \frac{p^2}{2} + \left(\frac{x^2}{2} - J \right) e^{-ax^2} \quad (30)$$

to our energy curve. Then by complex-scaling method, the internal coordinates of the Hamiltonian is dilated by a complex factor $\eta = \alpha e^{-i\theta}$ such that $H(x) \rightarrow H(x/\eta) \equiv H_\eta(x)$. We can solve the complex eigenvalue of $H_\eta(x)$ by the method D or using our previous method [36].

6. Conclusion

In this study we have compared several recently proposed quantum algorithms when used to compute the electronic state energies of the water molecule. These methods include first-order Trotter-PEA method based on the first-order Trotter decomposition, first- and second-order Direct-PEA methods based on direct implementation of the truncated propagator, Direct Measurement method based on direct implementation of the Hamiltonian and Pairwise PEA method, a VQE algorithm with a designed ansatz.

After deriving the Hamiltonian of the water molecular using the STO-3G basis set, we have explained in detail how each method works and derived their qubit requirements, gate complexities and measurement scalings. We have also calculated the ground state energy of the water molecular and shown the ground energy curves from all five methods. All methods are able to provide

an accurate result. We have compared these methods and concluded that the second-order Direct-PEA provides the most efficient circuit implementations in terms of gate complexity. With large scale quantum computation, the second-order direct method seems to better suit large molecule systems. In addition, since Pairwise VQE requires the least qubit number, it is the most practical method for near-term applications on the current available quantum computers.

Moreover, we have applied our PEA-type methods and Direct Measurement method to solve excited state energy curves for water molecule. The fifth excited state energy curve implies shape resonance. We have introduced recent work on quantum algorithms for solving the molecular resonance problems and given two possible ways to solve the water molecule resonance properties, including our Direct Measurement method which is able to solve the problem efficiently.

Acknowledgments

This material is based upon work supported by the U.S. Department of Energy, Office of Basic Energy Sciences, under Award Number DE-SC0019215. Author Daniel Murphy acknowledges the support of NSF REU award PHY-1460899.

Disclosure statement

No potential conflict of interest was reported by the authors.

References

- [1] S. Kais, *Quantum Information and Computation for Chemistry: Advances in Chemical Physics*, Vol. 154 (Wiley Online Library, NJ, 2014), p. 224109.
- [2] R.P. Feynman, *Int. J. Theor. Phys.* **21**, 467–488 (1982).
- [3] S.B. Bravyi and A.Y. Kitaev, *Ann. Phys.* **298**, 210–226 (2002).
- [4] K. Setia and J.D. Whitfield, *J. Chem. Phys.* **148**, 164104 (2018).
- [5] M. Staudtner and S. Wehner, Lowering qubit requirements for quantum simulations of fermionic systems. arXiv preprint arXiv:1712.07067 (2017).
- [6] R. Xia, T. Bian, and S. Kais, *J. Phys. Chem. B* **122** (13), 3384–3395 (2017).
- [7] M. Troyer and U.-J. Wies, *Phys. Rev. Lett.* **94**, 170201 (2005).
- [8] S. Lloyd, *Science* **273**, 1073–1077 (1996).
- [9] D.S. Abrams and S. Lloyd, *Phys. Rev. Lett.* **79**, 2586 (1997).
- [10] A. Aspuru-Guzik, A.D. Dutoi, P.J. Love and M. Head-Gordon, *Science* **309**, 1704–1707 (2005).
- [11] J.D. Whitfield, J. Biamonte and A. Aspuru-Guzik, *Mol. Phys.* **109**, 735–750 (2011).
- [12] D. Wecker, B. Bauer, B.K. Clark, M.B. Hastings and M. Troyer, *Phys. Rev. A* **90**, 022305 (2014).
- [13] D.W. Berry, A.M. Childs, R. Cleve, R. Kothari and R.D. Somma, *Phys. Rev. Lett.* **114**, 090502 (2015).
- [14] G.H. Low and I.L. Chuang, Hamiltonian simulation by qubitization. arXiv preprint arXiv:1610.06546 (2016).
- [15] R. Babbush, N. Wiebe, J. McClean, J. McClain, H. Neven and G.K. Chan, Low depth quantum simulation of electronic structure. arXiv preprint arXiv:1706.00023 (2017).
- [16] A. Daskin and S. Kais, *Quantum Inf. Process.* **16**, 33 (2017a).
- [17] A. Daskin and S. Kais, Direct application of the phase estimation algorithm to find the eigenvalues of the Hamiltonians. arXiv preprint arXiv:1703.03597 (2017b).
- [18] A. Daskin and S. Kais, A generalized circuit for the hamiltonian dynamics through the truncated series. arXiv preprint arXiv:1801.09720 (2018).
- [19] A. Peruzzo, J. McClean, P. Shadbolt, M.-H. Yung, X.-Q. Zhou, P.J. Love, A. Aspuru-Guzik and J.L. O’Brien, *Nat. Commun.* **5**, 4213 (2014).
- [20] J.R. McClean, J. Romero, R. Babbush and A. Aspuru-Guzik, *New J. Phys.* **18**, 023023 (2016).
- [21] P.J.J. O’Malley, R. Babbush, I.D. Kivlichan, J. Romero, J.R. McClean, R. Barends, J. Kelly, P. Roushan, A. Tranter, N. Ding, B. Campbell, Y. Chen, Z. Chen, B. Chiaro, A. Dunsworth, A.G. Fowler, E. Jeffrey, E. Lucero, A. Megrant, J.Y. Mutus, M. Neeley, C. Neill, C. Quintana, D. Sank, A. Vainsencher, J. Wenner, T.C. White, P.V. Coveney, P.J. Love, H. Neven, A. Aspuru-Guzik and J.M. Martinis, *Phys. Rev. X* **6**, 031007 (2016).
- [22] A. Kandala, A. Mezzacapo, K. Temme, M. Takita, M. Brink, J.M. Chow, and J.M. Gambetta, *Nature* **549**, 242 (2017).
- [23] B. P. Lanyon, J.D. Whitfield, G.G. Gillett, M.E. Goggin, M.P. Almeida, I. Kassal, J.D. Biamonte, M. Mohseni, B.J. Powell, M. Barbieri, A. Aspuru-Guzik and A.G. White, *Nat. Chem.* **2**, 106–111 (2010).
- [24] R.P. Muller, Python quantum chemistry (pyquante) program (2009). [Online; accessed 16-March-2018]. <http://pyquante.sourceforge.net/>.
- [25] J.T. Seeley, M.J. Richard and P.J. Love, *J. Chem. Phys.* **137**, 224109 (2012).
- [26] S. Bravyi, J.M. Gambetta, A. Mezzacapo and K. Temme, Tapering off qubits to simulate fermionic hamiltonians. arXiv preprint arXiv:1701.08213 (2017).
- [27] H.F. Trotter, *Proc. Am. Math. Soc.* **10**, 545–551 (1959).
- [28] M. Suzuki, *Commun. Math. Phys.* **51**, 183–190 (1976).
- [29] I. Dhand and B.C. Sanders, *J. Phys. A Math. Theor.* **47**, 265206 (2014).
- [30] A.Y. Kitaev, Quantum measurements and the abelian stabilizer problem. arXiv preprint quant-ph/9511026 (1995).
- [31] M. Dobšíček, G. Johansson, V. Shumeiko and G. Wendin, *Phys. Rev. A* **76**, 030306 (2007).
- [32] D.W. Berry, A.M. Childs, R. Cleve, R. Kothari and R.D. Somma, in *Forum of Mathematics, Sigma* (Cambridge University Press, 2017), Vol. 5.
- [33] A. Gilyén, S. Arunachalam and N. Wiebe, Optimizing quantum optimization algorithms via faster quantum gradient computation. arXiv preprint arXiv:1711.00465 (2017).
- [34] J.I. Colless, V.V. Ramasesh, D. Dahlen, M.S. Blok, M.E. Kimchi-Schwartz, J.R. McClean, J. Carter, W.A. De Jong and I. Siddiqi, *Phys. Rev. X* **8**, 011021 (2018).
- [35] S. Sim, J. Romero, P.D. Johnson and A. Aspuru-Guzik, *Physics* **11**, 14 (2018).
- [36] A. Daskin, A. Grama and S. Kais, *Quantum Inf. Process.* **13**, 333–353 (2014).

- [37] H. Wang, L.-A. Wu, Y.-X. Liu and F. Nori, Phys. Rev. A **82**, 062303 (2010).
- [38] H. Terashima and M. Ueda, Int. J. Quantum Inf. **3**, 633–647 (2005).
- [39] B. Simon, Ann. Math. **97** (2), 247–274 (1973).
- [40] N. Moiseyev and C. Corcoran, Phys. Rev. A **20**, 814 (1979).
- [41] N. Moiseyev, P.R. Certain and F. Weinhold, Mol. Phys. **36**, 1613–1630 (1978).
- [42] N. Moiseyev, P. Froelich and E. Watkins, J. Chem. Phys. **80**, 3623–3628 (1984).
- [43] P. Serra, S. Kais and N. Moiseyev, Phys. Rev. A **64**, 062502 (2001).
- [44] A. Barenco, C.H. Bennett, R. Cleve, D.P. DiVincenzo, N. Margolus, P. Shor, T. Sleator, J.A. Smolin and H. Weinfurter, Phys. Rev. A **52**, 3457 (1995).
- [45] P.A. Ivanov, E.S. Kyoseva and N.V. Vitanov, Phys. Rev. A **74**, 022323 (2006).
- [46] S.S. Bullock, D.P. O’Leary and G.K. Brennen, Phys. Rev. Lett. **94**, 230502 (2005).
- [47] J. Urías and D.A. Quiñones, Can. J. Phys. **94**, 150–157 (2015).
- [48] M.A. Nielsen and I. Chuang, Quantum Computation and Quantum Information (2002), Cambridge University Press, New York.

Appendices

Appendix 1. H₂O Hamiltonian at equilibrium

Table A1. Spin-type Hamiltonian of the water molecule at equilibrium when O–H is 1.9 a.u.

IIIII	-72.008089	IIIIZ	0.373979	IIIIXX	-0.050755
IIIIYY	0.113535	IIIIZI	0.002526	IIIIZZ	0.779273
IIIIZI	-0.771553	IIIIZIZ	0.043092	IIIIZXX	0.113535
IIIIZYY	-0.050755	IIIIZZI	0.785287	IIIIZZZ	-0.030367
IIIXIX	0.009295	IIIXIXI	0.000158	IIIXIXZ	-0.009295
IIIXZXZ	-0.000158	IIIZIII	-0.373979	IIIZIIZ	-0.148141
IIIZIYY	-0.011744	IIIZIZZ	-0.146285	IIIZIIZ	0.141059
IIIZZXX	-0.011744	IIIZZZI	-0.136887	IXIIIX	0.000158
IXIIIXI	0.013400	IXIIZXZ	-0.000158	IXIXXZ	-0.013400
IXXIII	-0.050755	IYYIII	0.113535	IYYIIZ	0.011744
IYYIYY	0.019371	IYYIZZ	0.031747	IYYZII	-0.011216
IYYZXX	0.019371	IYYZZI	0.031561	IZIIII	-0.002526
IZXIIIX	0.009295	IZXIXI	0.000158	IZXIXZ	-0.009295
IZXZXZ	-0.000158	IZZIII	0.779273	IZZIIIZ	0.146285
IZZIYY	0.031747	IZZIZZ	0.220040	IZZIIIZ	-0.154863
IZZZXX	0.031747	IZZZZI	0.179396	XIIIXI	0.012412
XIIIXXX	-0.007950	XIIIXZI	0.012412	XIIXYX	0.007950
XXXXII	-0.007950	XXXXXX	0.018156	XXXXZI	-0.007950
XXXXYX	-0.018156	XXZXXZ	-0.006979	XXZYII	0.006979
XZIXII	-0.012412	XZIXXX	0.007950	XZIXZI	-0.012412
XZIXYX	-0.007950	YXYXII	0.007950	YXYXXX	-0.018156
YXYXZI	0.007950	YXYXYX	0.018156	YIIXXZ	-0.006979
YIYYII	0.006979	ZIIIII	0.771553	ZIIIIIZ	0.141059
ZIIIIYY	0.011216	ZIIIZZ	0.154863	ZIIZII	-0.154860
ZIIZXX	0.011216	ZIIZZI	0.146877	ZIZIII	0.043092
ZXXIII	-0.113535	ZXXIIZ	-0.011744	ZXXIYY	-0.019371
ZXXIIZ	-0.031747	ZXXZII	0.011216	ZXXZXX	-0.019371
ZXXZZI	-0.031561	ZXZIIIX	-0.000158	ZXZIXI	-0.013400
ZXZIZX	0.000158	ZXZZXZ	0.013400	ZYIIII	0.050755
ZZIIII	0.785287	ZZIIIZ	0.136887	ZZIYYI	0.031561
ZZIIZZ	0.179396	ZZIIZI	-0.146877	ZZIZXX	0.031561
ZZIZZI	0.189343	ZZZIII	0.030367		

Notes: There are 95 terms, and listed are each operator and corresponding coefficient. X,Y,Z,I stand for the spin matrices $\sigma^x, \sigma^y, \sigma^z$ and the identity operator on a single qubit subspace.

Appendix 2. Error analysis

A.2.1 Trotter PEA

The Trotter decomposition is

$$e^{-iHt} = \prod_{i=1}^L e^{-i\alpha_i h_i t} + O(A^2 t^2). \quad (\text{A1})$$

Suppose our input is an eigenstate of $|\varphi\rangle_s$ of the Hamiltonian and has $H|\varphi\rangle_s = E|\varphi\rangle_s$, then:

$$\begin{aligned} & \prod_{i=1}^L e^{-i\alpha_i h_i t} |\varphi\rangle_s \\ &= (e^{-iHt} - O(A^2 t^2)) |\varphi\rangle_s \\ &= (e^{-iEt} - O(A^2 t^2)) |\varphi\rangle_s + O(A^2 t^2) |\varphi^\perp\rangle \\ &= e^{-iEt} (1 - O(A^2 t^2) e^{iE}) |\varphi\rangle_s + O(A^2 t^2) |\varphi^\perp\rangle \\ &= e^{-iEt} (1 - O(A^2 t^2) - iO(A^2 t^2)) |\varphi\rangle_s + O(A^2 t^2) |\varphi^\perp\rangle \\ &= (1 - O(A^2 t^2)) e^{-iEt} e^{i \tan^{-1}(O(A^2 t^2)/(1 - O(A^2 t^2)))} |\varphi\rangle_s \\ &\quad + O(A^2 t^2) |\varphi^\perp\rangle \\ &= (1 - O(A^2 t^2)) e^{-i(Et + O(A^2 t^2))} |\varphi\rangle_s + O(A^2 t^2) |\varphi^\perp\rangle. \end{aligned} \quad (\text{A2})$$

It should be noticed that in this equation, $O(A^2 t^2)$ is an operator before being applied to $|\varphi\rangle_s$.

In this way, the possibility that we can measure the correct ground state energy is $1 - O(A^2 t^2)$. After 2^D gates, in which D represents the number of digits we want to measure by PEA, the probability of state $|0\rangle|\psi\rangle_s$ should be still large. By setting the final coefficient to be $1 - \frac{1}{8}$, then:

$$(1 - O(A^2 t^2))^{2^D} = 1 - \frac{1}{8}, \quad (\text{A3})$$

$$2^{-D} = O(A^2 t^2). \quad (\text{A4})$$

The error of the energy resulting from the phase is: $\epsilon_1 = O(A^2 t^2)$. If we use PEA until D digits, the error of the energy resulting from PEA is: $\epsilon_2 = O(2^{-D}/t) = O(A^2 t)$. Then totally we have an error: $\epsilon = O(\epsilon_1 + \epsilon_2) = O(A^2 t)$.

Since the error for the first-order Trotter–Suzuki decomposition is:

$$e^{-iHt} - \prod_{i=0}^L e^{-i(\alpha_i h_i t/2)} \prod_{i'=L}^0 e^{-i(\alpha_{i'} h_{i'} t/2)} = O(A^3 t^3), \quad (\text{A5})$$

by a similar analysis the total error after PEA based on Trotter–Suzuki decomposition would be $\epsilon = O(A^3 t^2)$.

A.2.2 Direct PEA (first order)

From the main part, after gate U_r , we obtain:

$$\begin{aligned} U_r |0\rangle_a |\psi\rangle_s &= \frac{\sqrt{1 + \frac{E^2}{\kappa^2}}}{s} e^{-i \tan^{-1}(E/\kappa)} |0\rangle_a |\psi\rangle_s + |\Phi_1^\perp\rangle \\ &= \frac{\sqrt{1 + \frac{E^2}{\kappa^2}}}{1 + \frac{A}{\kappa}} e^{-i \tan^{-1}(E/\kappa)} |0\rangle_a |\psi\rangle_s + |\Phi_1^\perp\rangle \end{aligned}$$

$$\begin{aligned}
&= p e^{-i \tan^{-1}(E/\kappa)} |0\rangle_a | \psi \rangle_s + \sqrt{1-p^2} | \Phi^\perp \rangle \\
&= \cos \theta e^{-i \tan^{-1}(E/\kappa)} |0\rangle_a | \psi \rangle_s + \sin \theta | \Phi^\perp \rangle.
\end{aligned} \tag{A6}$$

Here $A = \sum_{i=1}^{2^m-1} \beta_i = \sum_{i=1}^L |\alpha_i| \geq |E|$, $\theta = \arccos\left(\sqrt{1+E^2/\kappa^2}/(1+A/\kappa)\right)$.

To increase the probability of $|0\rangle_a | \psi \rangle_s$, we use $Q = U_r(U_0 \otimes I^{\otimes n})U_r^\dagger(U_0 \otimes I^{\otimes n})$ to do oblivious amplitude amplification:

$$\begin{aligned}
Q^N U_r |0\rangle_a | \psi \rangle_s &= (-1)^N \cos((2N+1)\theta) e^{-i \tan^{-1}(E/\kappa)} |0\rangle_a | \psi \rangle_s \\
&\quad + \sin((2N+1)\theta) | \Phi^\perp \rangle \\
&= p_f |0\rangle_a | \psi \rangle_s + \sqrt{1-p_f^2} | \Phi^\perp \rangle.
\end{aligned} \tag{A7}$$

The idea is, if κ is large, $\sqrt{1+E^2/\kappa^2}/(1+A/\kappa) \approx 1/(1+A/\kappa)$, and $\theta' = \cos^{-1}(1/(1+A/\kappa)) \approx \theta$. By choosing large N and κ to satisfy $(2N+1)\theta' = \pi$, which means $A/\kappa = 1/\cos(\pi/(2N+1)) - 1$, we are able to get $\cos((2N+1)\theta) \approx -1$.

Since:

$$\begin{aligned}
\theta - \theta' &= \cos^{-1}\left(\frac{\sqrt{1+\frac{E^2}{\kappa^2}}}{1+\frac{A}{\kappa}}\right) - \cos^{-1}\left(\frac{1}{1+\frac{A}{\kappa}}\right) \\
&= \frac{\sqrt{2}}{4} \eta^2 \left(\frac{A}{\kappa}\right)^{3/2} + O\left(\left(\frac{A}{\kappa}\right)^{5/2}\right).
\end{aligned} \tag{A8}$$

In which $\eta = |E/A| \leq 1$. Then after N rotations

$$\begin{aligned}
|p_f| &= |\cos((2N+1)\theta)| \\
&= \cos((2N+1)(\theta' - \theta)) \\
&= 1 - \frac{(2N+1)^2}{16} \eta^4 \left(\frac{A}{\kappa}\right)^3 + O\left(\left(\frac{A}{\kappa}\right)^4\right) \\
&= 1 - \frac{\pi^6}{2^{11}} \eta^4 \frac{1}{N^4} + O\left(\frac{1}{N^5}\right).
\end{aligned} \tag{A9}$$

This means if we set large enough N , and then set $\kappa = A \cos(\pi/(2N+1))/(1 - \cos(\pi/(2N+1)))$, we are able to amplify the probability of $|0\rangle_a | \psi \rangle_s$ to be as close to 1 as we want.

Now we are taking $U_q = Q^N U_r$ to encode the energy into the phase. For the next PEA step, if we would like D digit accuracy, we have to make sure after 2^D gates of U_q , the probability of state $|0\rangle_a | \psi \rangle_s$ is still large. To make the analysis easier, we set the final coefficient for that state $1 - 1/2^3$. Then the following formula should be satisfied:

$$|p_f|^{2^D} = 1 - \frac{1}{2^3} \tag{A10}$$

$$2^{-D} = \frac{\pi^6 \eta^4}{2^{11} \ln(\frac{8}{7})} \frac{1}{N^4} + O\left(\frac{1}{N^5}\right) \tag{A11}$$

$$D = \min \left\{ \log_2 \left(\frac{2^{11} \ln(\frac{8}{7})}{\pi^6 \eta^4} \right) + 4 \log_2 N \right\} \approx -1.81 + 4 \log_2 N. \tag{A12}$$

Since D-digit output from PEA gives us the phase φ to approximate $(1/2\pi) \tan^{-1}(-E/\kappa)$, and the error of the phase is 2^{-D} , we get the error of the energy to be:

$$\begin{aligned}
\epsilon &= \tan(2\pi * 2^{-D}) \times \kappa = \frac{\pi^5 \eta^4}{2^7 \ln(\frac{8}{7})} \frac{1}{N^2} + O\left(\frac{1}{N^3}\right) \\
&\approx \frac{17.90 \eta^4 A}{N^2} \leq \frac{17.90}{N^2} A.
\end{aligned} \tag{A13}$$

We can see that, by taking large N and set corresponding κ (which is also large), we are able to control the accuracy of PEA process.

A.2.3 Direct PEA (second order)

From the main part, after gate U_{2r} , we obtain:

$$\begin{aligned}
U_{r2} |00\rangle |0\rangle_a | \psi \rangle_s &= \frac{\sqrt{1+\frac{E^4 t^4}{4A^2}}}{1+t+\frac{t^2}{2}} e^{-i \tan^{-1}((Et/A)/(1+E^2 t^2/2A))} \\
&\quad |00\rangle |0\rangle_a | \psi \rangle_s + | \Psi_1^\perp \rangle \\
&= p e^{-i \tan^{-1}((Et/A)/(1+E^2 t^2/2A))} \\
&\quad |00\rangle |0\rangle_a | \psi \rangle_s + \sqrt{1-p^2} | \Psi^\perp \rangle \\
&= \cos \theta e^{-i \tan^{-1}((Et/A)/(1+E^2 t^2/2A))} \\
&\quad |00\rangle |0\rangle_a | \psi \rangle_s + \sin \theta | \Psi^\perp \rangle.
\end{aligned} \tag{A14}$$

Here $A = \sum_{i=1}^{2^m-1} \beta_i = \sum_{i=1}^L |\alpha_i| \geq |E|$, $\theta = \cos^{-1}\left(\frac{\sqrt{1+E^4 t^4/4A^2}}{1+t+t^2/2}\right)$.

Apply $Q_2 = U_{2r}(U_0^+ \otimes I^{\otimes n})U_{2r}^\dagger(U_0^+ \otimes I^{\otimes n})$, in which $U_0^+ = 2|00\rangle |0\rangle_a |0\rangle_{00} - I^{\otimes m+2}$, to do oblivious amplitude amplification:

$$\begin{aligned}
Q_2^N U_{2r} |00\rangle |0\rangle_a | \psi \rangle_s &= (-1)^N \cos((2N+1)\theta) e^{-i \tan^{-1}((Et/A)/(1+E^2 t^2/2A))} \\
&\quad |0\rangle_a | \psi \rangle_s + \sin((2N+1)\theta) | \Psi_{a+s+2}^\perp \rangle \\
&= p_f |00\rangle |0\rangle_a | \psi \rangle_s + \sqrt{1-p_f^2} | \Psi_{a+s+2}^\perp \rangle.
\end{aligned} \tag{A15}$$

Let $\theta' = \cos^{-1}(1/(1+t+t^2/2))$ and choose large N and small t to satisfy $(2N+1)\theta' = \pi$, which leads to

$$t = -1 + \sqrt{\frac{2}{\cos \frac{\pi}{2N+1}} - 1} = \frac{\pi^2}{8N^2} + O\left(\frac{1}{N^3}\right). \tag{A16}$$

Then:

$$\begin{aligned}
\theta - \theta' &= \cos^{-1}\left(\frac{\sqrt{1+\frac{E^4 t^4}{4A^2}}}{1+t+\frac{t^2}{2}}\right) - \cos^{-1}\left(\frac{1}{1+t+\frac{t^2}{2}}\right) \\
&= \frac{\sqrt{2}}{16} \eta^4 t^{7/2} + O(t^{9/2}).
\end{aligned} \tag{A17}$$

In which $\eta = |E/A| \leq 1$. Then after N rotations

$$\begin{aligned} |p_f| &= |\cos((2N+1)\theta)| \\ &= \cos((2N+1)(\theta' - \theta)) \\ &= 1 - \frac{(2N+1)^2}{16^2} \eta^8 t^7 + O(t^8) \\ &= 1 - \frac{\pi^{14}}{2^{27}} \eta^8 \frac{1}{N^{12}} + O\left(\frac{1}{N^{13}}\right). \end{aligned} \quad (\text{A18})$$

This means if we set large enough N , and then set $t = -1 + \sqrt{2/\cos(\pi/(2N+1)) - 1}$, we are able to amplify the probability of $|00\rangle_a |\psi\rangle_s$ to be as close to 1 as we want.

Now we are taking $U_{q2} = Q_2^N U_{r2}$ to encode the energy into the phase, if we would like D digit accuracy, we have to make sure after 2^D gates of U_{q2} , the probability of state $|0\rangle_a |\psi\rangle_s$ is still large. By setting the final coefficient is $1 - \frac{1}{2^3}$, then the following formula should be satisfied:

$$|p_f|^{2^D} = 1 - \frac{1}{2^3} \quad (\text{A19})$$

$$2^{-D} = \frac{\pi^{14} \eta^8}{2^{27} \ln(\frac{8}{7})} \frac{1}{N^{12}} + O\left(\frac{1}{N^{13}}\right) \quad (\text{A20})$$

$$\begin{aligned} D &= \min \left\{ \log_2 \left(\frac{2^{27} \ln(\frac{8}{7})}{\pi^{14} \eta^8} \right) + 12 \log_2 N \right\} \\ &\approx 0.974 + 12 \log_2 N. \end{aligned} \quad (\text{A21})$$

Since D -digit output from PEA gives us the phase φ to approximate $-(1/2\pi) \tan^{-1}((Et/A)/(1 + E^2 t^2/2A))$ and the error of phase is 2^{-D} , we get the error of the energy E to be:

$$\epsilon = \frac{\pi^{13} \eta^8}{2^{23} \ln \frac{8}{7}} \frac{A}{N^{10}} + O\left(\frac{A}{N^{11}}\right) \approx \frac{2.59 \eta^8 A}{N^{10}} \leq \frac{2.59}{N^{10}} A. \quad (\text{A22})$$

We can see that by taking large N and set corresponding small t , we are able to control the accuracy of PEA process.

A.2.4 Direct measurement

After applying the gate U'_r :

$$U'_r |0\rangle_a |\psi\rangle_s = \frac{E}{A} |0\rangle_0 |\psi\rangle_s + |\Phi_1^\perp\rangle. \quad (\text{A23})$$

We obtain eigenenergy of state $|\psi\rangle_s$ by calculating probability of the wanted state: $|0\rangle_a |\psi\rangle_s$. The standard error of E by X measurements is:

$$\sigma = \frac{|E|}{\sqrt{X}} \sqrt{1 - \frac{E^2}{A^2}}. \quad (\text{A24})$$

Appendix 3. Complexity

A.3.1 Trotter PEA

We need n qubits for the state and at least 1 qubit for PEA process, so totally we need $O(n)$ qubits.

If we measure the ground state energy to D bit precision, we need $O(2^D L n)$ standard gates to implement PEA, in which by saying standard gates we mean single qubit gates and CNOT gates. Since $2^D = O(1/A^2 t^2) = O(A^2/\epsilon^2)$, and for molecular

system, $L = n^4$, so the gate complexity of Trotter PEA would be $O(n^5/(\epsilon/A)^2)$.

For PEA based on the second-order Trotter–Suzuki decomposition, we still need $O(2^D L n)$ standard gates. Now $2^D = O(1/A^3 t^3) = O(A^{1.5}/\epsilon^{1.5})$, so the gate complexity would be $O(n^5/(\epsilon/A)^{1.5})$.

A.3.2 Direct PEA (first order)

To do Direct PEA, we need n qubits to represent the system state and $m = \lceil \log_2(L) \rceil$ qubits to represent the ancilla state. We also need at least 1 qubit for multi-control Toffoli gates in B gate construction [44]. Towards molecular system of $L = O(n^4)$, so the number of required qubits is $O(n)$.

To meet properties of B, we can use Householder transformation and set it as:

$$B = I - \frac{2}{\langle u|u_a \rangle} |u\rangle\langle u_a|, \quad (\text{A25})$$

where $|u\rangle_a = B|0\rangle_a - |0\rangle_a$. The complexity of constructing this gate has been analysed before [17,45–47]. Since Givens rotation $G_{L-2,L-1}(\theta_{L-1})$ can nullify $B_{0,L-1}$, it can also nullify all $B_{j,L-1}$ for $j \neq L-1$ and update $B_{L-1,L-1}$ to 1 due to B 's special form. And $G_{L-2,L-1}^T(\theta_{L-1})$ would nullify all $B_{L-1,j}$ except $B_{L-1,L-1}$. For index smaller than $L-1$ but larger than 1, we can do the same thing. Finally we can choose $G_{1,1}(\theta_1)$ to update last 4 elements of B and obtain an identity matrix. Thus we have:

$$G_{1,1}(\theta_1) \prod_{i=2}^{L-1} G_{i-1,i}(\theta_i) B \prod_{i=L-1}^2 G_{i-1,i}^T(\theta_i) = I, \quad (\text{A26})$$

$$B = \prod_{i=L-1}^2 G_{i-1,i}^T(\theta_i) G_{1,1}^T(\theta_1) \prod_{i=2}^{L-1} G_{i-1,i}(\theta_i). \quad (\text{A27})$$

In this way, B gate can be obtained as a product of $2L-3$ Givens rotation matrices. Since each Givens rotation matrix can be achieved by at most m m -control Toffoli gates, which would cost $O(m^2)$ standard gates [44,48] each, totally $O(Lm^3) = O(L \log^3 n)$ gates are required. For $select(V)$ gate, we need $O((n+m)L)$ standard gates. In this way, U_r requires $O(L \log^3 n + (n+m)L) = O(n^5)$ gates. U_0 only needs $O(m)$ standard gates, so Q also requires $O(n^5)$ standard gates, which leads the gate complexity of U_q to be $O(Nn^5)$. Since $N = O(1/(\epsilon/A)^{1/2})$, PEA for D digit accuracy would result in a total of $O(2^D N n^5) = O(n^5/(\epsilon/A)^{2.5})$ standard gates.

A.3.3 Direct PEA (second order)

We need n qubits to represent the system state, $m' = \lceil \log_2(L) \rceil + 2$ qubits to represent the ancilla state. So the number of required qubits is still $O(n)$ as the first-order direct PEA.

When constructing U_{r2} , gate U_r takes $O(n^5)$ standard gates, gate P takes $O(L) = O(n^4)$ standard gates, B_2 , B_2^\dagger and phase gate $e^{-i(\pi/2)}$ only takes a small constant of standard gates. So the gate complexity of U_{r2} is still $O(n^5)$. Q_2 also requires $O(n^5)$ standard gates since U_0^\dagger needs $O(m)$ standard gates. Since $N = O(1/(\epsilon/A)^{0.1})$, PEA for D digit accuracy would result in a total of $O(2^D N n^5) = O(n^5/(\epsilon/A)^{1.3})$ standard gates.

A.3.4 Direct measurement

The number of required qubits for Direct Measurement Method is the sum of system and ancilla qubits: $O(n)$. Since only one U_r gate is enough, the complexity of the standard gates is $O(n^5)$. Since now the result of measurements is a binomial distribution, to measure the Energy E to accuracy(standard deviation) ϵ , we have to make $X = E^2/\epsilon^2$ measurements.

A.3.5 Variational quantum eigensolver

The number of qubits required for Pairwise VQE is n , and the gate complexity is $O(n^2d)$, where d is the number of

entangling gate layers. Assume we made X_i measurements for calculating $\langle h_i \rangle$, its accuracy (standard deviation) would be $\epsilon_i = 1/X_i$. With $X = \sum_{i=1}^L X_i$ measurements, the accuracy of Hamiltonian would be

$$\epsilon = \sum_{i=1}^L \frac{a_i}{\sqrt{X_i}} \leq \sqrt{\sum_{i=1}^L a_i^2} \sqrt{\sum_{i=1}^L \frac{1}{X_i}} \leq A \sqrt{\sum_{i=1}^L \frac{1}{X_i}}. \quad (\text{A28})$$

If $X_i = X/L$, we have $\epsilon \leq AL/\sqrt{X}$, then we need $X = A^2L^2/\epsilon^2 = A^2n^8/\epsilon^2$ measurements to achieve accuracy ϵ . Considering the number of iterations for optimisation, N_{iter} , the total number of measurements is $(A^2n^8/\epsilon^2)N_{\text{iter}}$.